

Published in final edited form as:

*Int J Radiat Biol.* 2011 October ; 87(10): 1001–1010. doi:10.3109/09553002.2011.556178.

## Specific issues in small animal dosimetry and irradiator calibration

Terry Yoshizumi<sup>1</sup>, Samuel L. Brady<sup>2</sup>, Mike E. Robbins<sup>3</sup>, and J. Daniel Bourland<sup>3</sup>

<sup>1</sup>Department of Radiology, Duke University, Durham, NC

<sup>2</sup>Medical Physics Graduate Program, Duke University, Durham, NC

<sup>3</sup>Department of Radiation Oncology, Wake Forest University School of Medicine, Winston-Salem, NC, USA

### Abstract

**Purpose**—In response to the increased risk of radiological terrorist attack, a network of Centers for Medical Countermeasures against Radiation (CMCR) has been established in the United States, focusing on evaluating animal model responses to uniform, relatively homogenous whole- or partial-body radiation exposures at relatively high dose rates. The success of such studies is dependent not only on robust animal models but on accurate and reproducible dosimetry within and across CMCR. To address this issue, the Education and Training Core of the Duke University School of Medicine CMCR organised a one-day workshop on small animal dosimetry. Topics included accuracy in animal dosimetry accuracy, characteristics and differences of cesium-137 and X-ray irradiators, methods for dose measurement, and design of experimental irradiation geometries for uniform dose distributions. This paper summarises the information presented and discussed.

**Conclusions**—Without ensuring accurate and reproducible dosimetry the development and assessment of the efficacy of putative countermeasures will not prove successful. Radiation physics support is needed, but is often the weakest link in the small animal dosimetry chain. We recommend: (i) A user training program for new irradiator users, (ii) subsequent training updates, and (iii) the establishment of a national small animal dosimetry center for all CMCR members.

### Keywords

small animal dosimetry;  $\gamma$ - and X-ray irradiators; irradiator calibration; radiation physics

### Introduction

The terrorist attacks on the World Trade Center and the Pentagon on September 11, 2001, provided a stark reminder of the potential risk of large-scale involvement of the civilian population in a radiological terrorist event. In response to this threat, a network of eight Centers for Medical Countermeasures against Radiation (CMCR) was established in the United States (US) in 2005 funded through the National Institute of Allergy and Infectious Diseases (NIAID) with National Cancer Institute (NCI) involvement. These CMCR were created to serve as multidisciplinary, extramural research centres comprised of academic,

© 2011 Informa UK, Ltd.

Correspondence: Dr J. Daniel Bourland, PhD, Department of Radiation Oncology, Wake Forest University School of Medicine, Medical Center Blvd, Winston-Salem, NC 27157, USA. Tel: + 1 (336) 713 6503. Fax: + 1 (336) 713 6622. bourland@wfubmc.edu.

#### Declaration of interest

The authors report no conflicts of interest. The authors alone are responsible for the content and writing of the paper.

commercial, and government laboratories focusing on a number of areas, including: (i) The development of agents for prophylaxis, mitigation, and treatment of radiation injury, and (ii) new or expanded educational resources to improve expertise in the radiation sciences, particularly radiation biology; a need previously acknowledged by the NCI and the American Society for Radiation Oncology (ASTRO) (Coleman et al. 2003).

The CMCR acknowledged the need for standardised animal model systems to identify and test new countermeasures, within a framework consistent with Food and Drug Administration (FDA) requirements. Building upon recommendations from an earlier NCI Workshop held in 2003 (Stone et al. 2004), the CMCR jointly sponsored a workshop, 'Animal Models for Medical Countermeasures' held on 18–19 January 2008 in San Antonio, Texas, USA (Williams et al. 2010). This report focused primarily on the most appropriate species and rodent strains to be used to assess countermeasure efficacy in particular organ systems. Although the need to consider other factors, including radiation quality and dosimetry was recognised, little detail as to the impact of these radiation physics-based factors on the biological response to radiation was included in this report.

The physical nature and characteristics of ionising radiation enable, in theory, the delivery of a defined dose of radiation to a well-defined target volume with accuracy in the order of 1 – 3%, a far smaller source of error than that observed in biological systems. Indeed, in the past decade technical advances in radiation oncology have led to a proliferation of sophisticated dose-shaping and delivery systems, including intensity-modulated radiation therapy, image-guided radiation therapy (IGRT), 3-dimensional conformal radiation therapy, stereotactic radiosurgery, tomotherapy, proton therapy, brachytherapy, etc. (Vikram et al. 2009). These advances have greatly improved the ability of radiation oncologists, working closely with radiation physicists, to image and verify delivery of more uniform, higher radiation doses to the tumour while sparing surrounding normal tissue (Berman and Rengan 2008, Gaspar and Ding 2008).

Although small animal image-guided irradiation systems are now commercially available, the vast majority of animal studies utilise simpler, less sophisticated irradiation devices such as orthovoltage X-ray machines, cesium-137 irradiators, or cobalt-60 irradiators. Indeed, given the CMCR-focus of evaluating animal models within the context of a response to a uniform, relatively homogenous whole- or partial-body exposure to moderate radiation doses at relatively high dose rates (Williams et al. 2010), it would appear that the irradiation component of any experiment would be essentially trivial. Such a conclusion is clearly wrong. Without ensuring accurate and reproducible dosimetry, the time, effort, and expense of carrying out experiments to develop and assess the efficacy of putative counter-measures is simply wasted. Despite this obvious conclusion, it would appear that little coordinated effort has gone into ensuring a standardised approach to radiation dosimetry across the CMCR.

To start to address this important challenge, the Education and Training Core of the Radiation Countermeasures Center of Research Excellence (RadCCORE, PI Nelson Chao, MD) based at the Duke University School of Medicine (DUSM) organised a one-day workshop for their members entitled, 'Small Animal Dosimetry: Current State and Future Directions' on 20 May 2010. The stated goal of the workshop was to derive uniform dosimetry methods across the various RadCCORE institutions (DUSM, Durham, NC, Oak Ridge National Laboratory, Oak Ridge, TN, University of Arkansas for Medical Sciences [UAMS], Little Rock, AK, University of North Carolina [UNC] at Chapel Hill, Chapel Hill, NC, and Wake Forest University Health Sciences [WFUHS], Winston-Salem, NC, USA). Topics included: (i) Why do we need accuracy in animal dosimetry?, (ii) what are the differences between cesium-137, cobalt-60, and X-ray irradiators?, and (iii) how do you

measure and get uniform doses from sources that have varying geometries and energy distributions? This was followed by a session equivalent to radiation physics 101 and a discussion in which various investigators presented their experiences and observations. Finally, a brainstorming session reviewed how to move forward with recommendations from the workshop and extend this exercise to other CMCR.

### Irradiation devices

Ionising radiation in the form of  $\gamma$  and X-rays, also called electromagnetic or photon radiation, can be produced through decay of a radionuclide or by electrical means. Irradiation devices for small animal irradiation exist based on either principle and include designs specific to the animal size as well as devices for diagnostic or therapeutic human uses or basic physics experiments that are adapted for animal irradiations. The  $\gamma$ - and X-ray penetration into tissue, called *beam quality*, depends on photon energy – higher energy photon radiation is more penetrating and will deposit dose at increased depths (Figure 1). Besides beam quality, radiation dose delivered depends on dose rate, irradiation time, size of the radiation field, distance from the source to the point of irradiation, and other physical parameters that may be device-specific. Table I lists research irradiator devices and some of their typical operating parameters, which are now discussed for their use in animal research.

### Self-shielded radionuclide irradiators

Radionuclide irradiators use one or more high activity sealed sources of a  $\gamma$ -emitting radionuclide, typically cesium-137 (one  $\gamma$  ray, energy = 0.662 MeV) or possibly cobalt-60 (two  $\gamma$  rays, energies = 1.17 MeV and 1.33 MeV), to create an irradiation field (Hranitzky et al. 1973, Howell et al. 1997, Brady et al. 2009). An irradiator cylindrical source is comprised of a chemically stable (e.g., salt or metal) form of the radionuclide encapsulated by a multi-walled steel cylinder that is sealed to prevent leakage of the radioactive material. The length of radioactive material, called the active length, is typically several centimeters long. The external dimensions of the source are larger than the active length because of the thickness of the (non-radioactive) encapsulation material. Either a single line source or a train of two or more linear sources can be used to provide a suitably-sized radiation field for small animal irradiations. Typical source activities of up to  $10^{14}$  Bq (1 Bq = 1 disintegration/s) provide nominal dose rates of 1 – 5 Gy/min depending on irradiator design (Table I). Thus, typical small animal doses of 2 – 10 Gy are delivered in 1 – 10 min. In a moving source irradiator, the source is stored in a shielded compartment that is attached to a shielded irradiation chamber (Figure 2A and 2B). The irradiation subject is placed in the correct position in the irradiation chamber and upon initiation of irradiation the source is moved from the shield by pneumatic or hydraulic means through a source guide tube (Figure 2B and 2C) to the irradiation position in the irradiation chamber. The linear radioactive source train is contained within the source guide and is not visible or accessible by the user. An end-to-end train of two 10 cm sources, with a ~ 10 cm gap between them, would move in the source guide tube from the source vault to the irradiation chamber to provide a suitable radiation field for the irradiator shown in Figure 2B. In a typical self-shielded irradiator the steel irradiator case and door contain 5 – 10 cm or more of lead or other equivalent shielding material for radiation protection of the operator. In this design the device can only initiate irradiation when the shielded access door is locked in the closed position. Thus, an operator can remain nearby the irradiator during operation. A timer set by the user controls the irradiation time, based on the desired dose and irradiation geometry. In a simpler design (not shown) the linear source stays in a shielded, fixed position at the rear of the device. A sample is placed into a holder and upon initiation of irradiation is rotated to the rear compartment where it is exposed to the source – neither the source nor the sample move during the irradiation time.

Moving source irradiators include either horizontal or vertical (Figure 2) motion of the source and large ( $50 \times 50 \times 50 \text{ cm}^3$ ) or small ( $20 \times 20 \times 20 \text{ cm}^3$ ) irradiation chambers with the guide tube and radiation source(s) in the center of the chamber or off to one side (or bottom for horizontal operation). Irradiation is accomplished using the full irradiation field (a 'flood' field) or the full field may be collimated to a specific field size by the use of a specially made or positioned collimating device. Depending on the geometry, the subject to be irradiated is placed on a platform or other location at a specified distance from the source. Replication of this positioning is very important to ensure consistent delivery of the desired dose and techniques for homogeneous dose deposition include rotating turntables placed on integrated drive shafts (Figure 2C), positioning the subject first on one side and then the other, or the use of beam filters to provide a uniform dose distribution. The basic dose distribution depends on the source, collimation and irradiation chamber designs, as well as the geometry and position of the irradiation subject, and this dose distribution must be validated for the experimental irradiation conditions.

### Kilovoltage and orthovoltage X-ray irradiators

Another commonly used irradiation device is the X-ray machine. This device produces X-rays through electronic means by the acceleration of electrons to hit a high atomic number ( $Z$ ) target to create *bremstrahlung* (braking) X-ray radiation. The X-ray machine can be turned ON or OFF using an electronic key switch. Main components include an X-ray tube (filament electron source and target) where the X-rays are produced, a collimating device to form an X-ray beam in one direction, a stand or other fixture to hold the X-ray tube, a high voltage generator, and a control system to set the X-ray beam energy, the tube current, and the irradiation time. In contrast to the  $\gamma$  irradiator, an X-ray beam is polyenergetic – the X-rays have energies from the maximum amount (which equals the electron acceleration energy, or the 'beam energy') down to zero. Kilovoltage X-ray irradiators operate from 10–120 kV (kilovolts), which compares with X-ray devices used for mammography (30–40 kV), dentistry (60 kV), and medical radiography (80–120 kV). Ortho-voltage X-ray irradiators operate from 130–320 kV. The higher X-ray energy requires a higher voltage generator and a heavy duty, water-cooled X-ray tube for high dose rate operation. The X-ray penetration and amount of dose near and at the surface depends on the X-ray energy (Figure 1). The range of X-ray energies enables a range of experimental subject sizes and conditions to be matched for the best possible uniform irradiation (Zoetelief et al. 1998, Wang et al. 2004, Medina et al. 2008). Dose rates from X-ray tubes vary based on system designs for low or high capacity. Specifically, X-ray dose rate,  $D$ , varies linearly with beam current (mA), as the square of the voltage (kV), and as the inverse-square of the distance (d). Thus,  $D \propto \text{mA} \times \text{kV}^2 \times 1/d^2$ . Typical dose rates are 1–3 Gy/min at 50 cm from the source.

### Megavoltage X-ray irradiators

High energy electron and X-ray beams from linear accelerators designed for clinical radiation treatment can be used for small and large animal irradiations (Williams and Hendry 1978, Gengozian et al. 1986, Chao et al. 2009). The megavoltage (MV) bremsstrahlung X-rays (6 – 18 MV) are produced in a high  $Z$  target after microwave acceleration of electrons in a waveguide assembly. Alternatively, the accelerated electron beam (6 – 20 MeV) can be used directly without creation of X-rays (Bourland 2006). Linear accelerators have high level positioning devices and a range of field sizes available that make a wide variety of experimental conditions possible. A wide range of field sizes ( $1 \times 1 \text{ cm}^2$  to  $40 \times 40 \text{ cm}^2$  or greater) and dose rates (1 – 6 Gy/min) are possible. For most small animal irradiations MV X-ray energies may be too high (Figure 1), resulting in too low surface dose, higher lateral scatter outside the field edge, and too high dose at depth. However, these characteristics can be controlled or accounted for by the particular experimental design.

Electron beams have a finite range and can be shaped for relatively homogeneous, unidirectional fields.

### Computed tomography devices for imaging and irradiation

Micro-computed tomography (micro-CT) imaging devices with small apertures and small focal spot X-ray tubes are available for small animal anatomic (structural) imaging (Schambach et al. 2010). These devices operate with the same principles of clinical CT devices, with specific designs for X-ray beam energy (20 – 60 kV or higher), low scatter and high spatial resolution (30 – 160  $\mu\text{m}$  or finer). Clinical CT devices have also been used for simultaneous imaging and dose delivery. Dose delivery depends on the imaging parameters such as field-of-view (FOV), X-ray tube energy, and beam current, as described earlier.

### Image-guided irradiation systems

Devices for small animal irradiations using image guidance have been developed for precision beam targeting that use imaging immediately prior to the irradiation (Stojadinovic et al. 2007, Wong et al. 2008, Saha et al. 2010). These devices replicate in miniature form the clinical devices being used for human IGRT (Jaffray 2007, Bourland 2008). Both X-ray CT imaging and irradiation are accomplished in the same device. Radiation dose characteristics are similar to kV and orthovoltage X-ray irradiators and must be characterised, particularly for the small fields used for irradiation. Focal stereotactic irradiation of small animals using a specialised clinical gamma unit (Kondziolka et al. 1992, Lunsford et al. 1990, DesRosiers et al. 2003, Wiandt et al. 2009) or linear accelerator (Spiegelmann et al. 1993, Solberg et al. 1994, Blatt et al. 1994) has also been performed.

### Radiation dose

Ionising radiation comprised of  $\gamma$ - and X-ray photons (high energy electromagnetic radiation) undergoes primarily atomic interactions in materials whereby energy carried by the radiation is transferred to the material (Bourland 2006). The initial interaction with an atomic electron breaks the electron bond, which leads to a small energy loss depending on the atomic number and electron binding energy, and the remaining energy is transferred to kinetic energy of the electron and possibly a scattered photon. Radiation dose,  $D$ , is the deposition of the electron kinetic energy over the relatively small volume of its ionisation path. The SI unit of dose,  $D$ , is the Gray (Gy) which has units of energy per mass (J/kg). Thus, radiation dose is the energy imparted (J) per unit mass of material (kg):  $1 \text{ Gray (Gy)} = 1 \text{ J/kg}$ . Besides the Gy, radiation dose is also represented by the rad:  $1 \text{ rad} = 100 \text{ erg/g}$ , and  $100 \text{ rad} = 1 \text{ Gy}$ . Air kerma ( $K_c$ ) is a quantity that is very similar to dose –  $K_c$  has the same units as dose (Gy) and is the amount of energy imparted (J) per unit mass of air (kg). The importance of air kerma is that dose to a material (e.g., experimental small animal) can be determined by measuring the air kerma,  $K_c$ , at the point where the animal will be irradiated. This measurement can be made with a radiation detector called an *ionisation chamber* (described below).

The consequences of irradiation and radiation dose occur in a stepwise fashion from physical interactions, chemical changes (broken bonds), biomolecular changes, and then tissue or organ responses. The amount of energy deposited in a radiation interaction is quite small – on average, there are 33.97 electron volts of energy deposited per ionising event (1 event = 1 ion pair = 1 ip), a quantity called the W-value ( $W = 33.97 \text{ eV/ip}$ ). In an ionising radiation field there are a very large number of quanta (photons and electrons) that include the incident radiation field and the subsequent secondary and scattered radiations that are created after the initial interaction. Radiation dose may be uniform because the incident radiation field or cumulative dose distribution is uniform. However, even with uniform radiation fluence, dose varies with the incident radiation energy and the atomic number and

density of the irradiated materials (e.g., lung, soft tissue, and bone) and at the interfaces of these materials (e.g., the external skin surface, and tissue-lung and tissue-bone interfaces). Such effects can be difficult to measure or calculate, especially for volumes having dimensions, <1 mm, and may or may not be important based on the irradiation geometry and the experimental design and goals. Microdosimetry techniques can be used to assess such non-homogenous dose distributions (Kellerer 1996, Walker 2006, Goodhead 2006) and include computational techniques such as Monte Carlo modeling (Wu et al. 2008, Marcelin et al. 2010).

### Radiation dosimeters for specific calibrations

In general two types of dose calibration data may be used in practice: (i) General dose rate calibration data for standardised reference geometry for the irradiator, and (ii) specific dose calibration data for a given setup geometry and radiation type. Type (i) calibration data are often provided by the manufacturers and will include the dose rate and possibly isodose curves at a given location. These data may not be directly applicable to specific irradiation geometries and should only be used as a guide, or to verify irradiator initial performance and subsequent quality assurance. Type (ii) calibration data describe the dose rate for the specific geometry (target dose and animal position) for the given animals (mice, rats, etc.) under specific radiation types (X-rays and gamma-rays). This is a critical piece of information for irradiating animals accurately and achieving the desired dose to a specified point or volume. Issues pertaining to the calibrations are described in more detail below.

Four main dosimeters are considered here for small animal irradiations as they are used in many laboratories; these include ionisation chambers, metal-oxide-semiconductor transistors (MOSFET), thermoluminescent dosimeters (TLD), and radiochromic films. Table II summarises published small animal dosimetry investigations using various dosimeters.

Ionisation chambers measure air kerma and dose with high accuracy and can be placed in an experimental radiation field at the intended location of a small animal for direct measurement of dose rate and dose. Tissue equivalent materials can be placed in a chamber to mimic an animal's body, or a small ionisation chamber can be wrapped in a protective sheath and inserted into a cadaver animal. While an ionisation chamber can be used for direct dose measurements, more commonly a reference class ionisation chamber is used to calibrate the response of other dosimeter types (e.g., MOSFET, TLD, and radiochromic films) in terms of the quantity air kerma (or dose). This calibration procedure should be performed for the radiation type and energy that will be used in the animal experiment. As a result of this calibration a calibration factor is used to convert the MOSFET, TLD, or radiochromic film dosimeter reading to a dose value for the irradiation device. Importantly, ionisation chambers serve as dosimetry standards and require X- and  $\gamma$ -ray energy-dependent calibration factors that are traceable to the National Institute of Standards and Technology (NIST). Low energy X-ray calibration factors for ionisation chambers are available (e.g., 60 – 300 kV X-rays) and at least one such calibrated ionisation chamber should be carefully maintained by an institution's health or medical physicist, to aid with animal irradiator calibrations.

The small size of the MOSFET and TLD detectors ( $1 \times 1$  to  $3 \times 3$  mm<sup>2</sup>) is a major advantage, enabling them to be inserted in the animal or phantom to measure local point or organ doses. Additional advantages for MOSFET detectors are near realtime readout capability and permanent storage of dose data. Disadvantages for MOSFET include: (i) Limited lifetime, (ii) sensitivity changes with irradiation history, and (iii) relatively high detector replacement cost. The major disadvantages of TLD detectors are the labour-intensive nature of (i) TLD preparation, (ii) TLD readout, and (iii) data processing. Radiochromic film has two advantages over conventional radiographic film of (i) not being

light sensitive, and (ii) not requiring a chemical development process. Instead, it is different from photographic or X-ray film and operates on the principle of polymerisation – the amount of polymerisation increases with radiation dose and changes the opacity of the film (increased dose causes increased film density).

Regardless of which detectors are used, the purpose of the calibration is to find the absorbed dose conversion factor to the target medium (water, air, etc.), for a given detector, (MOSFET, TLD etc.) with the given radiation beam quality, under various small animal irradiation geometries (partial organ irradiation, field size, distance, and sample rotation) (Ma et al. 2001).

### **Tissue equivalent phantoms for specific dosimetry**

Custom-designed tissue-equivalent mouse and rat phantoms are convenient ways to measure animal doses as well as to perform the irradiator output test in regularly-schedule intervals. Figure 3A – B shows tissue-equivalent mouse phantoms fabricated by the RADCCORE DUSM dosimetry group. the tissue-equivalent mouse phantom has three holes (front, middle and back) drilled for accepting either MOSFET or TLD detectors. Several mouse phantoms may be used in the mouse holder jig to obtain the average dose rates in a complex geometry as shown in Figure 3C. This geometry is often used in many cesium irradiators where multiple mice are placed in the jig on the rotating table to achieve uniform doses.

### **Specific calibration issues for two commonly used irradiators**

Orthovoltage X-ray units and radionuclide irradiators are commonly available small animal irradiation devices of relatively simple design that can safely be operated by individual researchers. Thus, after initial set-up for operation by vendor representatives and health or medical physicists, trained researchers are often the regular solo users of these two devices.

### **Orthovoltage X-rays**

As stated, typical orthovoltage X-ray irradiators may operate over a range of X-ray energies between 130 and 320 kV. In terms of protocol development, it is important to understand the following key parameters and resulting effects: (i) Dose rate as a function of beam energy, (ii) dose rate as a function of tube filtration, (iii) tissue attenuation as a function of tube filtration (beam quality), (iv) dose rate variation as a function of source-to-target distance (inverse square law), and (v) physical differences between orthovoltage X-ray and cesium-137 irradiator beam characteristics and dose rates. The beam energy (kV) represents the peak energy between the anode and cathode of the X-ray tube. It is important to note that the higher the kV, the higher the dose if all other parameters remain the same.

Interchangeable X-ray tube filters come with modern orthovoltage irradiators. The desired filter, essentially a thin metal slab (1 – 3 mm) is inserted in the X-ray tube housing and intercepts the X-ray beam as it exits the tube; it is important to decide which filter should be used for each experiment. Filters may be made of aluminum, tin, copper, and a combination of thereof. The filter and kV (beam energy) combination defines the hardness, or beam quality, of the X-ray beam, i.e., penetrability. Beam quality is expressed as half-value layer (HVL) in a standard material (usually aluminum or copper) at a given energy. A more penetrating beam has more uniform dose to deeper tissues and a larger HVL. However, the total number of emitted X-ray photons will decrease due to the added filtration. Therefore, it becomes a trade-off issue between the dose uniformity at depth and the irradiation time (dose rate). The choice of filter also affects the surface dose and the beam attenuation in tissue; the ‘softer’ X-rays are attenuated more than the ‘harder’ X-rays and surface dose is typically higher for a softer beam. If irradiating superficial tissues, an aluminum (low attenuation) filter or possibly no filter may suffice, but if the goal is to treat a deeper tissue, it may be necessary to select a more attenuating (thicker) beam filter that results in a harder

X-ray beam. There are two options available to increase the dose rate for a given filter, i.e., shorten the source-to-surface distance (SSD) or increase the tube-current time product. There is also an inverse square relationship between the radiation output and SSD. Finally it is important to note that cesium-137 irradiators have an advantage of providing far more penetrating  $\gamma$  rays than any orthovoltage X-ray beam (662 keV  $\gamma$  rays vs. 320 kV X-rays). As a result, care must be taken if changing the irradiator from cesium-137 to X-rays, or vice versa, since penetration depths as well as dose rates will be different. Researchers often report discrepancies in their small animal radiation response data without realising important differences between the two irradiators. It is important to understand the complete dosimetry picture whenever changing irradiators and it is important to consult and seek physics support from the outset of experimental design.

### Cesium-137 irradiator

Regardless of the manufacturer's design for a cesium-137 irradiator (static source, moving source with horizontal or vertical motion) the following parameters are important to achieve accurate dosimetry: (i) Initial dose rate (output) measurements for subsequent quality assurance, (ii) verification of the isodose map, (iii) dose rate measurements for specific experimental set-ups, (iv) correction of the reference dose rate for radioactive decay, and (v) annual quality assurance plan. We will discuss three key items for maintaining a high quality dosimetry program.

**(i) Initial acceptance testing**—A concept and practice of performing acceptance test of a new irradiator may not be well-rooted in most radiation biology laboratories today; however, the practice of acceptance testing is of vital importance and is no different from that of clinical radiation oncology practice where a qualified medical physicist performs an acceptance test of new equipment before commissioning for clinical use. Thus, an initial acceptance test of a  $\gamma$  irradiator should be established and performed by a qualified physicist. It is not the purpose of this paper, however, to describe a detailed method of each acceptance test for various irradiators that are currently in use. Any findings from the acceptance test should be reviewed based on the pre-established criteria by the physicist. If the performance falls below acceptable standards, corrective actions should be taken to achieve proper and expected device performance.

**(ii) Isodose mapping**—Although many manufacturers may provide isodose curves for their irradiators, this information should be checked and validated against one's own measurements. This is because many manufacturers provide pre-measured template isodose curves from the same model. Previous work by Brady et al. (2010) developed a method for irradiator isodose map quality assurance (QC) with no turntable rotation (static QC). The static QC methodology was not compatible with the manufacturer provided data, but demonstrated the usefulness of radiochromic Gaf-Chromic™ EBT film (International Specialty Products, Wayne, NJ, USA) as a quick and accurate QC dosimeter.

Rotation QC was recently developed as a new methodology at DUMC to provide a quick means of QC for a gamma irradiator (JS Shepherd Model Mark I, JL Shepherd and Associates, San Fernando, CA, USA) used for rotational specimens. A custom-made plastic film holder (Figure 4) was designed to attach onto current rotational platforms (see below) to provide QC at each position (Figure 2, positions 1 – 3). The film holder cylinder was designed to provide for proper charge particle equilibrium (CPE) for radiochromic EBT dosimetry. The results of isodose curves obtained using the film and those supplied by the manufacturer are shown in Figures 5 and 6. The shape of the dose distribution demonstrates that the irradiator design uses two 10 cm linear sources separated by a ~ 10 cm gap. The regions of cumulative highest dose occur at the periphery as the film rotates on the turntable



through a very high dose rate field close to the source in the guide tube (Figure 2B and C). As can be seen, the independently-measured isodose curves matched well with the manufacturer's isodose curves. Additionally, vertical (Figure 3A and C) and horizontal (Figure 3B and D) line profiles were plotted for positions 1 – 2 to demonstrate the measured isodose curves and those provided by the manufacturer; the line profiles agreed reasonably well. Thus, this film dosimetry method confirmed proper operation of the irradiator and can be used as part of an on-going cesium-137 irradiator quality assurance program.

**(iii) Dose rate decay corrections**—Cesium-137 has a half-life of 30.07 years, decaying by  $\beta$ -minus to a metastable nuclear isomer of barium-137, which has a half-life of 2.55 min and is responsible for all of the  $\gamma$  ray emission. The annual activity correction for exponential decay is 2.3% and this decay correction (a multiplying factor of 0.977) should be applied to the reference calibrated dose rate on a per-year basis.

## Conclusions and recommendations

The recent creation of the CMCR network has highlighted the need for uniformity in not only the animal model systems used to identify and test new countermeasures but also the quality and dosimetry of the irradiation used during animal exposure. Recommendations on the most appropriate species and strains to be used for assessing countermeasure efficacy in specific organ systems have been published by the CMCR (Williams et al. 2010). In contrast, little coordinated effort has gone into ensuring a standardised approach to radiation dosimetry across the CMCR. Commonly used  $\gamma$ - and X-ray irradiators are robust devices that can be used in a variety of experimental conditions and easily operated by laboratory personnel. However, technical and logistical challenges exist for the determination of individual dose calibration factors prior to various experimental set-ups, and the physics support required for this phase is often the weakest link in the small animal dosimetry chain. Unfortunately, the lack of physics support is a norm rather than exception in many of the US small animal radiation research facilities.

Dose rates and homogeneity of the radiation experimental fields should be determined by a qualified medical or radiation physicist, including consultation on the experimental goals and the design of the experimental irradiation geometry. Such expertise may be collectively shared by local physicists based on the irradiator device being used ( $\gamma$ - or X-ray irradiator, CT, micro-CT, linear accelerator, etc.) and each physicist's area of expertise. While irradiators have various levels of ease of operation, a user training program must be established for new users and subsequent web-based update training may be given. In addition,  $\gamma$  irradiators, with their high activity radioactive sources, have become a national security issue under the US Nuclear Regulatory Commission (NRC) and all users must accept Federal Bureau of Investigation (FBI) criminal background checks and fingerprinting in order to obtain access to the irradiator. This requirement for heightened radiological security will continue in the future.

It is of paramount importance to establish central oversight and establish a networking relationship among biology and physics consortium members. Within RadCCORE our cross-discipline and cross-institution interactions are resulting in the exchange of new ideas and transfer of knowledge between different member institutions. Our model is still a work-in-progress; however, we are achieving uniformity in the physics quality assurance program, and strongly recommend pursuing the establishment of a national small animal dosimetry centre for all CMCR members.

## Acknowledgments

### Notice of Acknowledgement

This paper Specific Issues in Small Animal Dosimetry and Irradiator Calibration, was supposed to be part of the Special Issue published in August 2011 titled “Overview of research from the Centers for Medical Countermeasures against Radiation”. Due to an error on the part of the publishers, the paper was omitted. The publisher wishes to apologize to the authors and readers for any inconvenience caused.

We wish to thank the participants in the “Small Animal Dosimetry: Current State and Future Directions” Workshop held on 20 May 2010. These include: Marjan Boerma (UAMS), June Brickey, Rita-Marie McFadden, Adeb Rahman (UNC Chapel Hill), Xiuhong Cao, John Chute, Divino Deoliveira, Rat Gunasingha, Lauren Jackson, Irene Li, Sarah Meadows, Ross McGurk, Qiong Qiu, Julie Sullivan, Greta Tonecheva, Minsi Zhang, Ping Zhang (DUMC) and Tom Seed. Special thanks to Joel Ross, PhD, for organising the Workshop. This work was supported by National Institutes of Health grant U19AI067798.

## References

- Berman AT, Rengan R. New approaches to radiotherapy as definitive treatment for inoperable lung cancer. *Seminars in Thoracic and Cardiovascular Surgery*. 2008; 20:188– 197. [PubMed: 19038727]
- Blatt DR, Friedman WA, Bova FJ, Theele DP, Mickle JP. Temporal characteristics of radiosurgical lesions in an animal model. *Journal of Neurosurgery*. 1994; 80:1046– 1055. [PubMed: 8189260]
- Bourland, JD. Radiation oncology physics. In: Gunderson, LL.; Tepper, JE., editors. *Clinical radiation oncology*. 2. Philadelphia, PA: WB Saunders Company; 2006.
- Bourland, JD. Image-guided radiation treatment. In: Wolbarst, AB.; Mossman, KL.; Hendee, WR., editors. *Advances in medical physics*. Madison, WI: Medical Physics Publishing; 2008.
- Brady SL, Toncheva G, Dewhurst MW, Yoshizumi TT. Characterization of a  $^{137}\text{Cs}$  irradiator from a new perspective with modern dosimetric tools. *Health Physics*. 2009; 97:195– 205. [PubMed: 19667802]
- Brady S, Gunasingha R, Yoshizumi TT, Howell C, Crowell A, Fallin B, Tonchev AP, Dewhurst MW. A feasibility study using radiochromic films for passive fast neutron 2D dosimetry. *Physics in Medicine and Biology*. 2010; 55:4977– 4992. [PubMed: 20693612]
- Chao TC, Chen AM, Tu SJ, Tung CJ, Hong JH, Lee CC. The evaluation of 6 and 18 MeV electron beams for small animal irradiation. *Physics in Medicine and Biology*. 2009; 54:5847– 5860. [PubMed: 19741277]
- Coleman CN, Stone HB, Alexander GE, Barcellos-Hoff MH, Bedford JS, Bristow RG, Dynlacht JR, Fuks Z, Gorelic LS, Hill RP, Joiner MC, Liu FF, McBride WH, McKenna WG, Powell SN, Robbins ME, Rockwell S, Schiff PB, Shaw EG, Siemann DW, Travis EL, Wallner PE, Wong RS, Zeman EM. Education and Training for Radiation Scientists: Radiation Research Program and American Society of Therapeutic Radiology and Oncology Workshop, Bethesda, Maryland, May 12 – 14. *Radiation Research*. 2003; 160:729– 737. [PubMed: 14640790]
- DesRosiers C, Mendonca MS, Tyree C, Moskvina V, Bank M, Massaro L, Bigsby RM, Caperall-Grant A, Valluri S, Dynlacht JR, Timmerman R. Use of the Leksell Gamma Knife for localized small field lens irradiation in rodents. *Technology in Cancer Research and Treatment*. 2003; 2:449– 454. [PubMed: 14529310]
- Figueroa SD, Winkelmann CT, Miller WH, Volkert WA, Hoffman TJ. TLD assessment of mouse dosimetry during microCT imaging. *Medical Physics*. 2008; 35:3866– 3874. [PubMed: 18841837]
- Gaspar LE, Ding M. A review of intensity-modulated radiation therapy. *Current Oncology Reports*. 2008; 10:294– 299. [PubMed: 18778554]
- Gengozian N, Taylor T, Jameson H, Lee ET, Good RA, Epstein RB. Radiation-induced hemopoietic death in mice as a function of photon energy and dose rate. *Radiation Research*. 1986; 105:320– 327. [PubMed: 3961097]
- Goodhead DT. Energy deposition stochastics and track structure: What about the target? *Radiation Protection and Dosimetry*. 2006; 122:3– 15.

- Howell RW, Goddu SM, Rao DV. Design and performance characteristics of an experimental cesium-137 irradiator to simulate internal radionuclide dose rate patterns. *Journal of Nuclear Medicine*. 1997; 38:727– 731. [PubMed: 9170437]
- Hranitzky EB, Almond PR, Suit HD, Moore EB. A cesium-137 irradiator for small laboratory animals. *Radiology*. 1973; 107:641– 644. [PubMed: 4702541]
- Jaffray DA. Image-guided radiation therapy: from concept to practice. *Seminars in Radiation Oncology*. 2007; 17:243– 244. [PubMed: 17903701]
- Kellerer AM. Radiobiological challenges posed by microdosimetry. *Health Physics*. 1996; 70:832– 836. [PubMed: 8635908]
- Kondziolka D, Lunsford LD, Claassen D, Maitz AH, Flickinger JC. Radiobiology of radiosurgery: Part I. The normal rat brain model. *Neurosurgery*. 1992; 31:271– 279. [PubMed: 1513433]
- Lin MD, Toncheva G, Nguyen G, Kim S, Anderson-Evans C, Johnson GA, Yoshizumi TT. Applications of MOSFET detectors for dosimetry in small animal radiography using short exposure times. *Radiation Research*. 2008; 170:260– 263. [PubMed: 18666818]
- Lunsford LD, Altschuler EM, Flickinger JC, Wu A, Martinez AJ. In vivo biological effects of stereotactic radiosurgery: A primate model. *Neurosurgery*. 1990; 27:373– 382. [PubMed: 1700326]
- Ma C, Liu C, Cogfey C, Nath R, Seltzer S, Seuntjens J. AAPM protocol for 40 – 300 kV x-ray beam dosimetry for radiotherapy and radiobiology. *Medical Physics*. 2001; 28:868– 893. [PubMed: 11439485]
- Marcelin B, Kjäll P, Johansson J, Lundin A, Nordström H, Eriksson M, Bernard C, Régis J. Using Monte-Carlo-simulated radiation transport to calculate dose distribution in rat before irradiation with Leksell Gamma Knife 4C: Technical note. *Stereotactic and Functional Neurosurgery*. 2010; 88:208– 215. [PubMed: 20460950]
- Medina LA, Herrera-Penilla BI, Castro-Morales MA, García-López P, Jurado R, Pérez-Cárdenas E, Chanona-Vilchis J, Brandan ME. Use of an orthovoltage X-ray treatment unit as a radiation research system in a small animal cancer model. *Journal of Experimental and Clinical Research*. 2008; 27:57.
- Saha D, Watkins L, Yin Y, Thorpe P, Story MD, Song K, Raghavan P, Timmerman R, Chen B, Minna JD, Solberg TD. An orthotopic lung tumor model for image-guided microirradiation in rats. *Radiation Research*. 2010; 174:62– 71. [PubMed: 20681800]
- Schambach SJ, Bag S, Schilling L, Groden C, Brockmann MA. Application of micro-CT in small animal imaging. *Methods*. 2010; 50:2– 13. [PubMed: 19706326]
- Solberg TD, De Salles AA, Hovda D, Holly FE. A universal, multi-modality localization system for animal radiosurgery. *Acta Neurochirurgica Supplement*. 1994; 62:28– 32. [PubMed: 7717131]
- Spiegelmann R, Friedman WA, Bova FJ, Theele DP, Mickle JP. LINAC radiosurgery: An animal model. *Journal of Neurosurgery*. 1993; 78:638– 644. [PubMed: 8450338]
- Stojadinovic S, Low DA, Hope AJ, Vicic M, Deasy JO, Cui J, Khullar D, Parikh PJ, Malinowski KT, Izaguirre EW, Mutic S, Grigsby PW. MicroRT-small animal conformal irradiator. *Medical Physics*. 2007; 34:4706– 4716. [PubMed: 18196798]
- Stone HB, Moulder JE, Coleman CN, Ang KK, Anscher MS, Barcellos-Hoff MH, Dynan WS, Fike JR, Grdina DJ, Greenberger JS, Hauer-Jensen M, Hill RP, Kolesnick RN, Macvittie TJ, Marks C, McBride WH, Metting N, Pellmar T, Purucker M, Robbins ME, Schiestl RH, Seed TM, Tomaszewski JE, Travis EL, Wallner PE, Wolpert M, Zaharevitz D. Models for evaluating agents intended for the prophylaxis, mitigation and treatment of radiation injuries. Report of an NCI Workshop, December 3 – 4, 2003. *Radiation Research*. 2004; 162:711– 728. [PubMed: 15548121]
- Vikram B, Coleman CN, Deye JA. Current status and future potential of advanced technologies in radiation oncology. Part 1. Challenges and resources. *Oncology (Williston Park)*. 2009; 23:279– 283. [PubMed: 19418829]
- Walker AJ. Techniques for radiation measurements: Microdosimetry and dosimetry. *Radiation Protection and Dosimetry*. 2006; 122:369– 373.
- Wang J, Zheng H, Ou X, Albertson CM, Fink LM, Herbert JM, Hauer-Jensen M. Hirudin ameliorates intestinal radiation toxicity in the rat: Support for thrombin inhibition as strategy to minimize side-

- effects after radiation therapy and as countermeasure against radiation exposure. *Journal of Thrombosis and Haemostasis*. 2004; 2:2027– 2035. [PubMed: 15550035]
- Wiant D, Atwood TF, Olson J, Papagikos M, Forbes ME, Riddle DR, Bourland JD. Gamma knife-radiosurgery treatment planning for small animals using high-resolution 7T micro-magnetic resonance imaging. *Radiation Research*. 2009; 172:625– 631. [PubMed: 19883231]
- Williams JP, Brown SL, Georges GE, Hauer-Jensen M, Hill RP, Huser AK, Kirsch DG, Macvittie TJ, Mason KA, Medhora MM, Moulder JE, Okunieff P, Otterson MF, Robbins ME, Smathers JB, McBride WH. Animal models for medical countermeasures to radiation exposure. *Radiation Research*. 2010; 173:557– 578. [PubMed: 20334528]
- Williams PC, Hendry JH. The RBE of megavoltage photon and electron beams. *British Journal of Radiology*. 1978; 51:220. [PubMed: 415786]
- Wong J, Armour E, Kazanzides P, Iordachita I, Tryggestad E, Deng H, Matinfar M, Kennedy C, Liu Z, Chan T, Gray O, Verhaegen F, McNutt T, Ford E, DeWeese TL. High-resolution, small animal radiation research platform with x-ray tomographic guidance capabilities. *International Journal of Radiation Biology, Oncology, Physics*. 2008; 71:1591– 1599.
- Wu L, Zhang G, Luo Q, Liu Q. An image-based rat model for Monte Carlo organ dose calculations. *Medical Physics*. 2008; 35:3759– 3764. [PubMed: 18777935]
- Zoetelief J, Wagemaker G, Broerse JJ. Dosimetry for total body irradiation of rhesus monkeys with 300 kV X-rays. *International Journal of Radiation Biology*. 1998; 74:265– 272. [PubMed: 9712556]

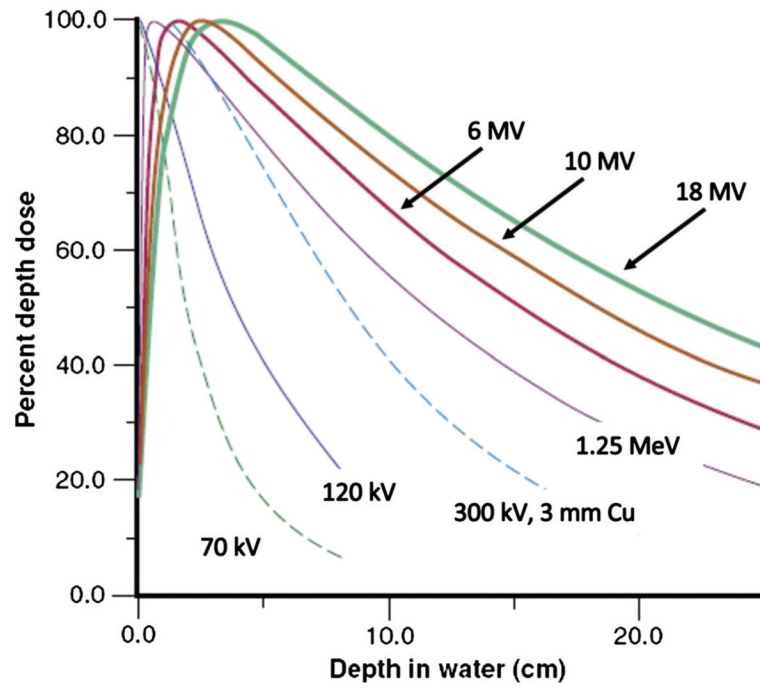


**Figure 1.** Diagnostic and megavoltage photon beam percent depth dose curves (from Bourland 2006, used with permission).

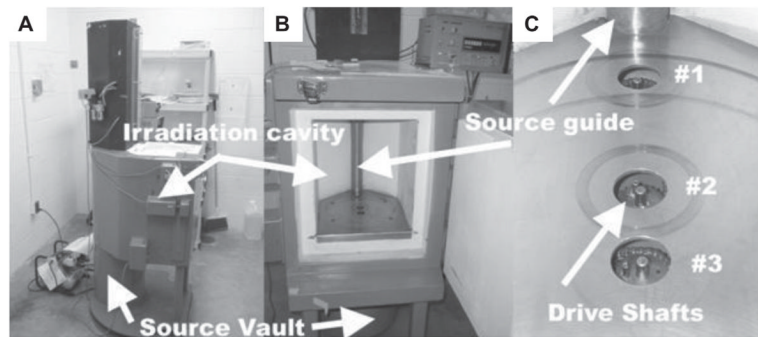


**Figure 2.**

Moving source gamma irradiator, vertical source orientation. A linear  $\gamma$  source moves from the shielded source vault (A) and (B) (bottom to top) to the shielded irradiation chamber (cavity). The source is enclosed by the tube seen in (B). A rotating platter can be mounted on sample driveshaft locations (#1, #2, and #3) to provide rotation for dose homogeneity. A timer mechanism controls the irradiation time, ending with the return of the sources to the shielded source vault.

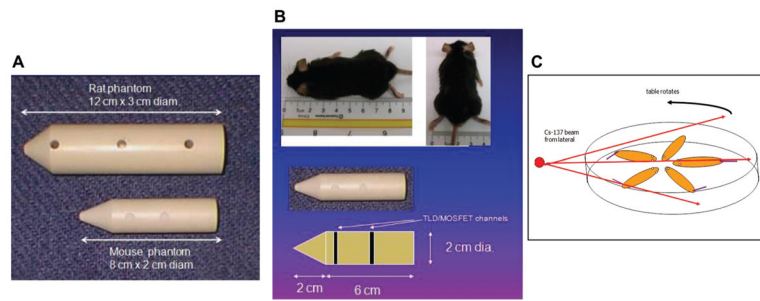


**Figure 3.** Tissue-equivalent rodent phantoms for irradiator dosimetry. (A) Rat and mouse phantoms with holes for dosimeter placement. (B) Phantom dimensions relative to animal. (C) Rotation platter used in irradiator (Figure 2) for dosimetry as well as experiment.

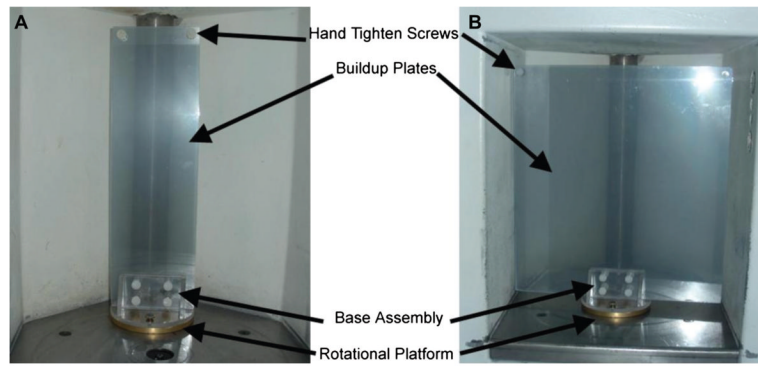


**Figure 4.**

Jig design: Rotation film stage assembly was designed to attach to a rotational platform provided by the manufacturer. A sandwich of two 2 mm thick Plexiglas plates was used to provide structural support and to establish proper charged particle equilibrium for the film. Two Plexiglas plate sizes were designed to be interchangeable with the base assembly for positions 1, 2, or 3 (Figure 2C): (A) small 10 cm wide plates for measurements at position 1 closest to the cesium-137 source and (B) large 30 cm wide plates for isodose curve measurements at positions 2 and 3.



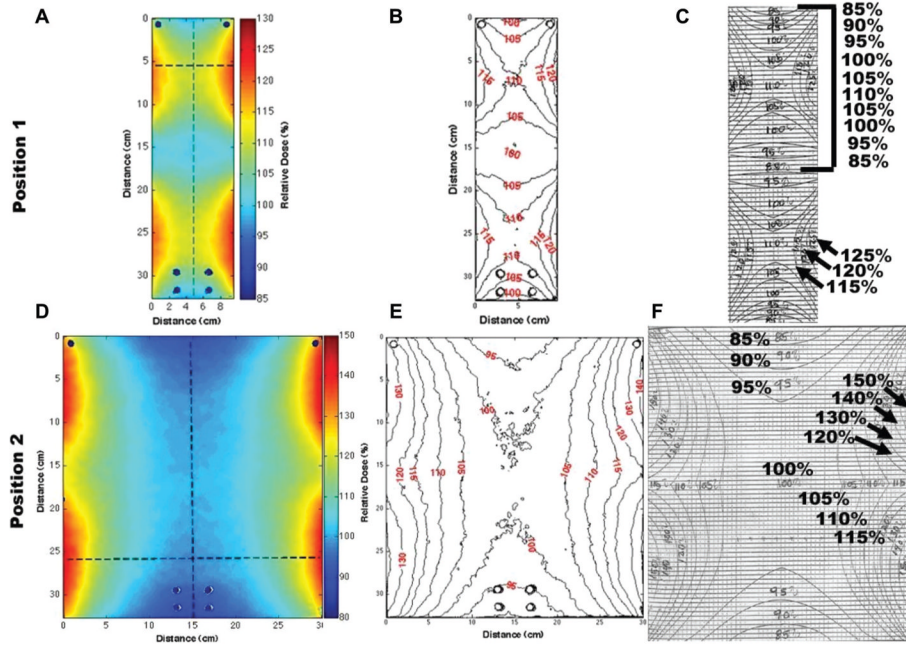


**Figure 5.**

Left column (A and D): Radiochromic film dose distributions are shown in colour wash for positions 1 and 2 (Figure 2C). Middle column (B and E): Dose distributions were converted to isodose curves. Right column (C and F): Manufacturer's isodose curves. Comparison of measured and manufacturer's isodose curve shows good agreement and verifies proper irradiator performance. The vertical axis (y-axis) represents the distance from the floor of the irradiator housing.

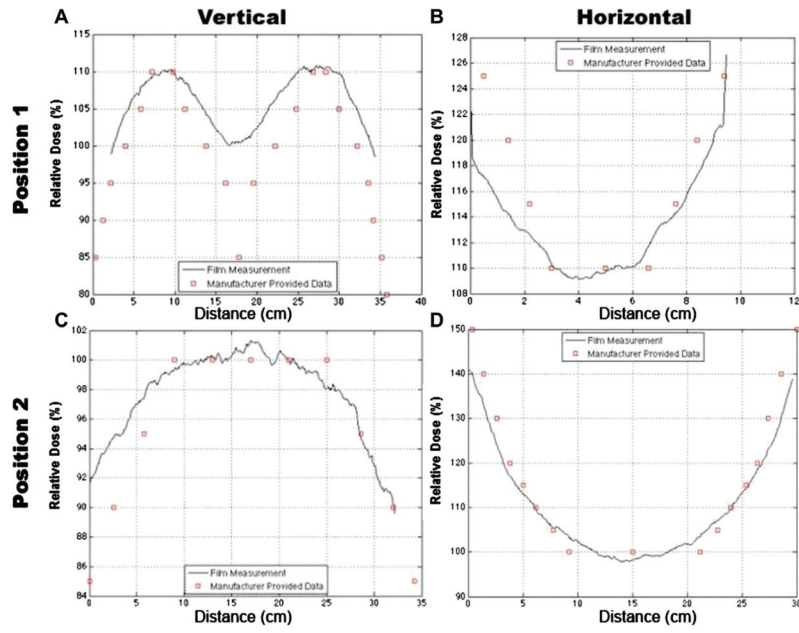


**Figure 6.**

Vertical and horizontal line dose profiles were obtained along the dotted lines in Figure 5A and D, and plotted with the corresponding manufacturer provided data for positions 1 – 2, respectively. Comparison of measured and manufacturer’s line dose profiles shows good agreement and verifies proper irradiator performance.

**Table I**

Small animal research irradiation devices and operating parameters.

Device	Radiation source (Energy)	Dose rate	Small animal applications	Comments
Radionuclide irradiator	Cesium-137 gamma ( $\gamma$ ) rays (0.662 MeV $\gamma$ ray) Less common: Cobalt-60 gamma ( $\gamma$ ) rays (1.17 and 1.33 MeV $\gamma$ rays) Both designs use linear, steel-encapsulated radioactive sources. A timer controls the irradiation time.	1 – 5 Gy/min @ defined positions within irradiation chamber. Nominal radioactivity of 2,000 Curies (Ci). Dose rate varies with source-to-sample distance and dose distribution uniformity may vary across the irradiated volume depending on sample size and position in the irradiation chamber.	Whole-body irradiation. Partial-body irradiations using specially-designed collimators. Irradiation of one or more animals possible, depending on size and geometry.	Simple design makes for ease of use. Source moves from the shielded condition to irradiate a chamber with enclosed sample. Designs are horizontal or vertical operation. Irradiation geometry can be customized for required experimental conditions. Dose rate calibration required to determine irradiation times. Radiological security must be insured.
X-Ray Tube	X rays (30 – 320 kV X-rays) Note: Orthovoltage X-ray energy range is 130– 320 kV. A timer controls the irradiation time.	1 – 5 Gy/min at 50 cm from source. Dose rate varies with energy (kV), filtration, source-to-sample distance, and tube (beam) current.	Whole-body irradiation. Partial-body or single-organ irradiations using collimated fields. Irradiation of one or more animals possible, depending on size and geometry.	A variety of beam energies is possible with depths of penetration from 0 – 2 cm. Can be used in single- or opposed-field geometries. Field sizes can be collimated to a specific size. Requires either a shielded enclosure or a shielded room. Dose rate calibration required to determine irradiation times.

**Table II**

Published dosimetry investigations for small animal radiation research.

<b>Animals (reference)</b>	<b>Machine</b>	<b>Detectors and additional tools</b>	<b>Comments</b>
Mouse (Figuroa et al. 2008)	microCT	Ion chamber, TLD-100	Implanted TLDs measured organ doses in brain, flank, bladder, kidney, GI, stomach liver, lung, and heart.
Tissue equivalent mouse phantom (Lin et al. 2008)	Digital subtraction angiography X-ray system	Ion chamber, TLD-100, MOSFET	MOSFET technology verified with TLD method.
Brady et al. 2009	cesium-137 irradiator	Ion chamber, TLD, radiochromic film dosimeters	Modern dosimetric tools to characterise cesium-137 irradiator